STEM CELLS AND DEVELOPMENT
Volume 19, Number 6, 2010

DOI: 10.1089/scd.2009.0184

Na^+/Ca^{2+} Exchanger is a Determinant of Excitation–Contraction Coupling in Human Embryonic Stem Cell–Derived Ventricular Cardiomyocytes

Ji-Dong Fu,[1,2] Peng Jiang,[1,2] Stephanie Rushing,[1,2] Jing Liu,[1,2] Nipavan Chiamvimonvat,[3] and Ronald A. Li[1,2,4–6]

In adult cardiomyocytes (CMs), the Na^+/Ca^{2+} exchanger (NCX) is a well-defined determinant of Ca^{2+} homeostasis. Developmentally, global NCX knockout in mice leads to abnormal myofibrillar organization, electrical defects, and early embryonic death. Little is known about the expression and function of NCX in human heart development. Self-renewable, pluripotent human embryonic stem cells (hESCs) can serve as an excellent experimental model. However, hESC-derived CMs are highly heterogeneous. A stably lentivirus-transduced hESC line (MLC2v-dsRed) was generated to express dsRed under the transcriptional control of the ventricular-restricted myosin light chain-2v (MLC2v) promoter. Electrophysiologically, dsRed+ cells differentiated from MLC2v-dsRed hESCs displayed ventricular action potentials (AP), exclusively. Neither atrial nor pacemaker APs were observed. While $I_{Ca\text{-}L}$, I_f, and I_{Kr} were robustly expressed, I_{Ks} and I_{K1} were absent in dsRed+ ventricular hESC-CMs. Upon differentiation (7+40 to +90 days), the basal $[Ca^{2+}]_i$, Ca^{2+} transient amplitude, maximum upstroke, and decay velocities significantly increased ($P < 0.05$). The $I_{Ca\text{-}L}$ antagonizer nifedipine (1 μM) decreased the Ca^{2+} transient amplitude (to ~30%) and slowed the kinetics (by ~2-fold), but Ca^{2+} transients could still be elicited even after complete $I_{Ca\text{-}L}$ blockade, suggesting the presence of additional Ca^{2+} influx(es). Indeed, Ni^{2+}-sensitive I_{NCX} could be recorded in 7+40- and +90-day dsRed+ hESC-CMs, and its densities increased from -1.2 ± 0.6 pA/pF at −120 mV and 3.6 ± 1.0 pA/pF at 60 mV by 6- and 2-folds, respectively. With higher $[Ca^{2+}]_i$, 7+90-day ventricular hESC-CMs spontaneously but irregularly fired transients upon a single stimulus under an external Na^+-free condition; however, without extracellular Na^+, nifedipine could completely inhibit Ca^{2+} transients. We conclude that I_{NCX} is functionally expressed in developing ventricular hESC-CMs and contributes to their excitation–contraction coupling.

Introduction

Loss of non-regenerative, terminally differentiated cardiomyocytes (CMs) is irreversible; moreover, myocardial repair is hampered by a severe shortage of donor cells and organs. Self-renewing pluripotent human embryonic stem cells (hESCs) can differentiate in vitro into all 3 primitive germ layers and their derivatives, including CMs [1]. Human ESC–derived CMs (hESC-CMs) display molecular, structural, and functional properties of early developing human fetal CMs [1,2]. Therefore, hESC-CMs may provide an unlimited ex vivo source of genuine human CMs for transplantation and can also serve as an excellent experimental model for studying human cardiogenesis. However, current protocols for cardiac differentiation of hESCs lead to a heterogeneous population of pacemaker-, atrial-, and ventricular-like derivatives, which are conventionally functionally classified based on their signature action potential (AP) profiles [1,3]. Indeed, we previously demonstrated that in vivo transplantation of a node of electrically active hESC-CMs, containing a mixture of ventricular, atrial, and nodal cells, into the ventricle can collectively induce a local epicardial pacing origin [2].

[1]Human Embryonic Stem Cell Consortium, [2]Department of Cell Biology and Human Anatomy, [3]Department of Internal Medicine, University of California, Davis, California.
[4]Institute of Pediatric Regenerative Medicine, Shriners Hospital for Children of North America, Sacramento, California.
[5]Stem Cell and Regenerative Medicine Program, Heart, Brain, Hormone and Healthy Aging Research Center and [6]Division of Cardiology, Department of Medicine, University of Hong Kong, Hong Kong, People's Republic of China.

Sarcolemmal Na^+/Ca^{2+} exchanger (NCX), a bidirectional transporter that catalyzes the exchange of 3 or 4 Na^+ ions for one Ca^{2+} ion, is a well-defined determinant of Ca^{2+} homeostasis [4]. NCX is responsible for extruding the elevated Ca^{2+} during contraction, thereby restoring a low resting $[Ca^{2+}]_i$ and a high excitation–contraction (E-C)-coupling gain. As one of the earliest functional gene products, NCX is known to be involved in embryonic heart development and function. Developmentally, global knockout of NCX in transgenic mouse models has been reported to lead to abnormal myofibrillar organization, apoptosis, electrical defects, and early embryonic death [5,6]. However, little is known about the expression and functional profiles of NCX in human heart development. We have previously reported that NCX is expressed at the protein level by western blot analysis in mixed hESC-CMs directly differentiated from hESCs by embryoid body formation [7]. But it remains uncertain whether NCX is functional. As such, their biophysical properties and contribution to E-C coupling are unknown. Since I_{NCX} measurements require the inhibition of most ion channels (such as K^+, Ca^{2+}, and Cl^- channels) and chamber-specific CMs differ significantly in their ion channel expression profiles, it will be necessary to identify and select the ventricular derivative for experiments to avoid ambiguities. In the present study, we generated an engineered hESC line whose ventricular derivatives were fluorescently labeled, followed by patch-clamp recording of I_{NCX} and functionally assessing its contribution to cytosolic Ca^{2+} transients and E-C coupling.

Materials and Methods

hESC culturing and differentiation

The H1 (WiCells, Madison, WI) hESC line (NIH code: WA01) chosen for this study were cultured and differentiated as we previously described [2,7]. In brief, H1 cells were grown on irradiated mEFs from 13.5-day embryos of CF-1 mice and trypsin-propagated. The culture medium consisted of 80% DMEM, 20% knockout serum replacement, 4 ng/mL basic fibroblast growth factor (b-FGF), 1 mmol/L glutamine, 0.1 mmol/L β-mercaptoethanol, and 1% nonessential amino acid solution (all from Invitrogen, Carlsbad, CA). For differentiation, hESCs were induced to form embryoid bodies (EBs). Undifferentiated cells were detached using 1 mg/mL type IV collagenase (Gibco-BRL, Carlsbad, CA) and transferred to Petri dishes with differentiation media containing 80% DMED, 20% fetal bovine serum defined (HyClone, Logan, UT), 1 mmol/L glutamine, and 1% nonessential amino acid without b-FGF. The aggregates were cultured in suspension for 7 days, followed by plating on gelatin-coated (0.1%; Sigma-Aldrich, St. Louis, MO) 60-mm dishes to form hESC-CMs.

Lentivirus-mediated gene transfer

For stable genetic modification, lentivirus (LV)-mediated gene transfer was performed as we previously reported [2]. To generate pLV-MLC2v-dsRed, a 250-bp fragment of the MLC2v promoter carrying the homologous sequence also found in rat and human, which has been shown to sufficiently recapitulate the cardiac-specific expression pattern [8–10], along with a 406-bp region of the human cytomegalovirus (CMV) enhancer and the dsRed gene, were inserted into the 3′ end of the plasmid pLV-EF1α-GFP at the *Bam*HI and *Cla*I restriction sites. EF1α-GFP was kept for selecting positively transduced undifferentiated hESCs. For generating LV particles, the plasmids pΔ8.91, pMD.G, and pLV-MLC2v-dsRed (3:1:2 mass ratio) were co-transfected into HEK293T cells seeded at a density of 6×10^6 cells per 10-cm dish 24 h prior to transfection. LV particles were harvested from the supernatant at 24 and 48 h post-transfection and stored at −80°C before use. For transduction, LV particles with a titer of 10^6 and an MOI of 3 and polybrene (6 μg/mL) were incubated with cells. A single round of LV transduction typically yields an efficiency of >50%.

Isolation of hESC-CMs

For isolating hESC-CMs, $dsRed^+$ outgrowths were microsurgically dissected from EBs at 2 stages, 7+30-to-40 days (40-day) and 7+80-to-90 days (90-day), by a glass knife [7,11] (cf. Fig. 1). The dissected clusters were digested with collagenase II (1 mg/mL) at 37°C for 30 min. The isolated cells were incubated with KB solution containing (mM): 85 KCl, 30 K_2HPO_4, 5 $MgSO_4$, 1 EGTA, 2 Na_2-ATP, 5 pyruvic acid, 5 creatine, 20 taurine, 20 D-glucose, at room temperature for 30 min. After plating on laminin-coated glass coverslips for 1 h at 37°C, culture media was added cautiously. To purify $dsRed^+$ hESC-CMs, cells were identified by their epifluorescence and sorted by MoFlo (Dako, Ft. Collius, CO).

Isolation of human fetal ventricular cardiomyocytes (FLV-CMs)

Human fetal ventricular cardiomyocytes (FLV-CMs) were isolated and experimented according to protocols approved by the UC Davis IUPAC and IRB (Protocol #200614787-1). In brief, fetal human hearts (16–18 weeks, Advanced Bioscience Resources, Inc. Alameda, CA) were perfused with enzymatic solutions using a customized Langendorff apparatus as previously described [7]. FLV-CMs were cultured in laminin-coated 24-well dishes with a density of ~5×10^5 cells/well with media containing: 5 mM carnitine, 5 mM creatine, 5 mM taurine, 100 μg/mL penicillin–streptomycin, and 10% fetal bovine serum in Medium 199 (Sigma-Aldrich Corp., St. Louis, MO).

Immunostaining

Cells were fixed for 15 min at room temperature with 4% paraformaldehyde in PBS. After washing with PBS, cells were permeabilized in PBS containing 0.2% Triton X-100, then incubated with primary mouse anti-MLC2v or anti-MLC2a monoclonal antibody. Alexa Fluor-647 anti-mouse IgG (Invitrogen) was the second antibody used for fluorescence imaging. Hoechst 33342 (H3570; Invitrogen) was used to stain the nuclei. Coverslips were mounted onto glass slides in Prolong Gold antifade reagent (Invitrogen). Samples were imaged on a confocal laser scanning microscope (C1si, Nikon, Japan).

Electrophysiology

Electrophysiological experiments were performed using the whole-cell patch-clamp technique with an Axopatch 200B amplifier and the pClamp9.2 software (Axon

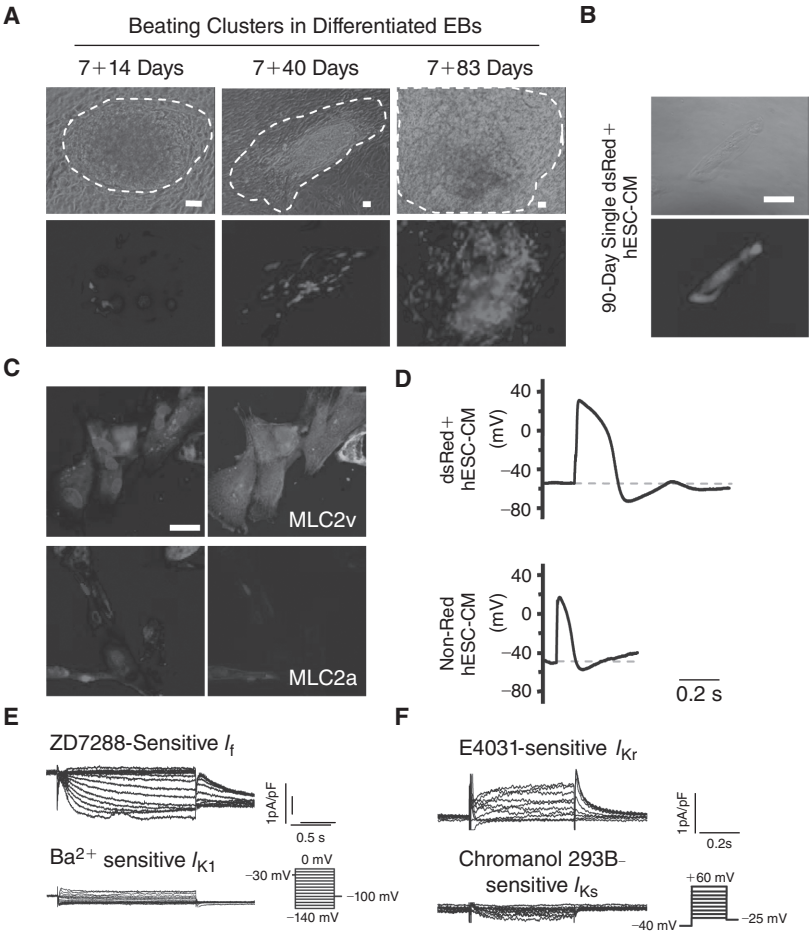

FIG. 1. DsRed+ cells differentiated from stably LV-MLC2v-dsRed-transduced human embryonic stem cells (hESCs) displayed a ventricular phenotype. (**A**) Representative images of MLC2v-dsRed hESCs differentiating embryoid bodies (EBs) at different stages. Beating areas are circled by dash lines. Bars represent 50 µm. (**B**) A representative single isolated and FACS-sorted 7+90-day dsRed+ hESC-cardiomyocytes (CMs). Bar indicates 20 µm. (**C**) dsRed+ cells were stained positively for MLC2v (upper) but not MLC2a staining (lower). Bar indicates 20 µm. (**D**) Typical ventricular action potential (AP) recorded from a single dsRed+ hESC-CM. Atrial AP could only be observed in non-dsRed hESC-CMs. (**E**) ZD7288-sensitive pacemaker current (I_f), but no I_{K1}, were expressed in dsRed+ hESC-CMs. (**F**) E4031-sensitive I_{Kr}, but not I_{Ks}, were expressed in dsRed+ hESC-CMs. Color images available online at www.liebertonline.com/scd.

Instruments Inc., Foster City, CA) as previously described [3]. A xenon arc lamp was used to view the dsRed fluorescence at 560/590 nm (excitation/emission). Patch pipettes were prepared from 1.5 mm thin-walled borosilicate glass tubes using a Sutter micropipette puller P-97 and had typical resistances of 4–6 MΩ. The micropipettes were filled with an internal solution containing (mmol/L): 110 K^+ aspartate, 20 KCl, 1 $MgCl_2$, 0.1 NaGTP, 5 MgATP, 5 Na_2-phospocreatine, 1 EGTA, 10 HEPES, pH adjusted to 7.3 with KOH. The external Tyrode's bath solution consisted of (mmol/L): 140 NaCl, 5 KCl, 1 $CaCl_2$, 1 $MgCl_2$, 10 glucose, 10 HEPES, pH adjusted to 7.4 with NaOH. For AP recording, current-clamp recordings were performed at 37°C within 24 to 48 h after hESC-CM isolation. The hESC-CMs were given a stimulus of 0.1–0.5 nA for 1–5 ms to elicit AP. Voltage-clamp recordings of ionic currents were performed using standard electrophysiological and pharmacological isolation.

For measuring the L-type Ca^{2+} currents ($I_{Ca\text{-}L}$), the internal solution contained (in mM): 130 CsCl, 1.0 $MgCl_2$, 0.1 NaGTP, 5 MgATP, 10 HEPES, and 10 EGTA. pH was adjusted to 7.2 with CsOH. The external solution contained (in mM): 136 NaCl, 5.4 CsCl, 1.0 $MgCl_2$, 2.0 $CaCl_2$, 2.0 NaH_2PO_4, 10 glucose, and 10 HEPES. pH was adjusted to 7.4 with NaOH, TTX (0.05 mM) and TEA-Cl (20 mM) were added during the recording, and $I_{Ca\text{-}L}$ was elicited by stepping to various voltages (−50 to +10 mV, 10 mV increments, 0.2 Hz) for 100 ms from a holding potential of −30 mV, and defined as 5 mM nifedipine-sensitive currents. Steady-state inactivation was determined by stepping to various pre-pulse voltages (−50 to +10 mV, 10 mV increments) for 1 s prior to depolarization to a fixed 250-ms test pulse of +10 mV every 10 s. Peak currents obtained at all voltages were normalized to the maximal value.

NCX current (I_{NCX}) density was determined using the whole-cell patch-clamp technique as described previously [12]. $[Ca^{2+}]_i$ was buffered to 150 nM with BAPTA (calculated using the Maxchelator program [13]). The external solution was K^+-free and contained (in mmol/L): Na^+ 135, Ca^{2+} 2, MgCl 1, glucose 10, HEPES 10, CsCl 10 (to block the inward rectifier K^+ current, I_{K1}, and the Na^+/K^+ pump), (in µmol/L): niflumic acid 100 (to block Ca^{2+}-activated Cl^- current), ouabain 10 (Na^+/K^+ pump inhibitor), and verapamil 10 (dihydropyridine antagonist), adjusted to pH 7.4 (CsOH). The internal solution contained (in mmol/L): CsCl 136, NaCl 10, aspartic acid 42, $MgCl_2$ 3, HEPES 5, tetraethylammonium (TEA) 20, MgATP 10, and 150 mM free $[Ca^{2+}]_i$, adjusted to pH 7.4 (CsOH). The holding potential was −30 mV to inactivate the T-type Ca^{2+} and Na^+ channels. Slow-ramp pulses were applied (+60 to −120 mV, 0.09 V/s) at 10 s intervals to construct the current−voltage (I/V) relationships. I_{NCX} was measured as the bidirectional Ni^{2+} (5 mM)-sensitive current.

Measurements of cytosolic Ca^{2+}

Intracellular Ca^{2+} transients were recorded from dsRed+ hESC-CMs as identified by fluorescence microscope, within 48 h after plating. A spectrofluorometric method with Fura-2/

AM as the Ca^{2+} indicator was used for measuring $[Ca^{2+}]_i$. dsRed+ hESC-CMs were incubated with 5 μM Fura-2/AM and 0.2% pluronic F-127 for 30 min at 37°C. Fluorescent signals obtained upon excitation at 340 nm (F_{340}) and 380 nm (F_{380}) were recorded from cells perfusing with Tyrode solution unless otherwise indicated. For Na^+-free solution, LiCl (140 mM) was used to replace NaCl (140 mM). The F_{340}/F_{380} ratio was used to represent cytosolic $[Ca^{2+}]_i$. To elicit cytoplasmic Ca^{2+} transients, hESC-CMs were electrically pulsed (0.1–0.5 Hz). Ca^{2+} transients were recorded and analyzed after a series of depolarization that enabled each transient to fully decay so as to establish a steady state. Data were analyzed using the Ionwizard software (Version 5, IonOptix) to generate the Ca^{2+} transient parameters reported [7,11,14].

Statistical analysis

All data were expressed as means ± SEM. One-way ANOVA followed by Newman-Keuls multiple comparison tests or paired *t*-test was carried out to test for differences between the mean values within the same study. A difference of $P < 0.05$ was considered significant.

Results

dsRed+ cells differentiated from stably LV-MLC2v-dsRed-transduced hESCs displayed a ventricular phenotype

To confirm the efficacy of LV-MLC2v-dsRed for identifying ventricular CMs, we first transduced and compared human fetal left ventricular (FLV) CMs and human embryonic kidney (HEK) 293 cells. FLV-CMs (but not HEK293 cells) uniquely expressed dsRed after LV-MLC2v-dsRed transduction (Supplementary Fig. 1A; Supplementary materials are available online at http://www.liebertpub.com/), indicating the cardiac specificity of our construct. We next generated the stably LV-MLC2v-dsRed-transduced (or MLC2v-dsRed) hESC line, whose karyotype was normal (Supplementary Fig. 1B). When undifferentiated, absolutely no dsRed+ cells could be detected (Supplementary Fig. 1C). For differentiation, MLC2v-dsRed hESCs were allowed to form EBs for 7 days, followed by plating on gelatin-coated culture dishes and observing for the appearance of beating clusters and dsRed expression. Same as untransduced control hESCs that we previously reported [2], spontaneously contracting clusters could be observed in EBs differentiated from LV-MLC2v-dsRed-transduced hESCs as soon as 10–14 days after plating (or 7+10–14 days). Furthermore, the percentage of EBs containing beating clusters was also not different (12% ± 2% from 10 batches). No dsRed+ cells could be observed until beating activities appeared. Indeed, not all beating cells were dsRed+ at Day 7+10-to-14. Figure 1A shows that dsRed+ cells significantly increased over time, with substantially more dsRed+ cells in 7+80-to-90-day EBs. Although dsRed+ cells were largely limited to the beating clusters at Day 7+40, some non-beating cells also became dsRed+ at Day 7+80-to-90.

For functional characterization, we dissected from EBs beating clusters that contained dsRed+ cells followed by dissociating them into single cells for electrophysiological recording. After FACS sorting, a typical single 90-day dsRed+ cell after attachment is shown in Figure 1B. As anticipated, dsRed+ cells were stained positively for the ventricular isoform (MLC2v), but not the atrial isoform (MLC2a), of the myosin light chain (Fig. 1C). Figure 1D further shows that functionally *only* ventricular-like action potentials (AP) could be recorded from 40-day dsRed+ cells ($n = 15$ of 15). In contrast, atrial-like APs were observed only in non-dsRed cells (5 of 7) isolated from the same beating clusters. The hyperpolarization-activated pacemaker current (I_f) and the rapid component of the delayed rectifier (I_{Kr}) were expressed in dsRed+ hESC-CMs; but the slow component (I_{Ks}) and the inward rectifier (I_{K1}) were not (Fig. 1E and 1F). These results were consistent with wild-type hESC-CMs that displayed ventricular APs. Therefore, dsRed+ cells differentiated from MLC2v-dsRed hESCs belonged to the ventricular lineage. Since cardiac differentiation of hESCs is known to generate a heterogeneous population of ventricular, atrial, and pacemaker derivatives [1,3], selection of dsRed+ hESC-CMs for experiments will enable us to study the ventricular lineage without ambiguities.

Development of Ca^{2+} transients during ventricular hESC-CM differentiation

Ca^{2+} homeostasis is crucial for E-C coupling and subsequently, the contractile properties of functioning CMs. Figure 2 summarizes the Ca^{2+} transient properties recorded from dsRed+ (ventricular) hESC-CMs at different time points upon differentiation. From 7+40 to 7+90-day post-differentiation, both the basal $[Ca^{2+}]_i$ and Ca^{2+} transient amplitude significantly increased ($P < 0.05$) (Fig. 2A–2C). Ca^{2+} transients of the 7+90-day group also had faster kinetics with higher maximum upstroke ($V_{max\text{-}upstroke}$; Fig. 2D) and maximum decay ($V_{max\text{-}decay}$; Fig. 2E) velocities ($P < 0.05$). Taken together, these results demonstrate that Ca^{2+} transients of ventricular hESC-CMs appeared to time-dependently mature in culture, although the adult level was still not reached even after almost 100 days.

Contribution of L-type Ca^{2+} channels to Ca^{2+} transients

In adult CMs, L-type Ca^{2+} ($I_{Ca\text{-}L}$) channels mediate the transport of trans-sarcolemmal Ca^{2+} influx for activating Ca^{2+} release from the sarcoplasmic reticulum (SR) via a process known as Ca^{2+}-induced Ca^{2+} release (CICR) during E-C coupling. In murine ESC-CMs, $I_{Ca\text{-}L}$ plays a similar functional role but the same in ventricular hESC-CMs has not been defined. Figure 3A and 3B shows that $I_{Ca\text{-}L}$ was robustly expressed in 7+40-day dsRed+ ventricular hESC-CMs (2.24 ± 0.54 pA/pF at +10 mV; $n = 4$). The steady-state activation ($V_{1/2} = -10.9 \pm 0.6$ mV, $K = 4.6 \pm 0.3$) and inactivation ($V_{1/2} = -27.1 \pm 2.0$ mV, $K = 7.6 \pm 1.3$) curves are given in Supplementary Figure 2. Upon infusion of nifedipine (1 μmol/L), a selective antagonist of $I_{Ca\text{-}L}$, the Ca^{2+} transient amplitude decreased to 33.5% ± 9.2% in 40-day ($n = 4$) and 28.0% ± 4.6% in 90-day ($n = 4$) dsRed+ ventricular hESC-CMs (Fig. 3C and 3D). The upstroke velocities of Ca^{2+} transients were significantly slowed (Fig. 3E). However, the inhibitory effect of nifedipine were not significantly different between 7+40-day and 7+90-day dsRed+ ventricular hESC-CMs ($P > 0.05$). Interestingly, Ca^{2+} transients, albeit small in the amplitude (Fig. 3C), could still elicited in both 7+40- and 7+90-day ventricular hESC-CMs even after $I_{Ca\text{-}L}$

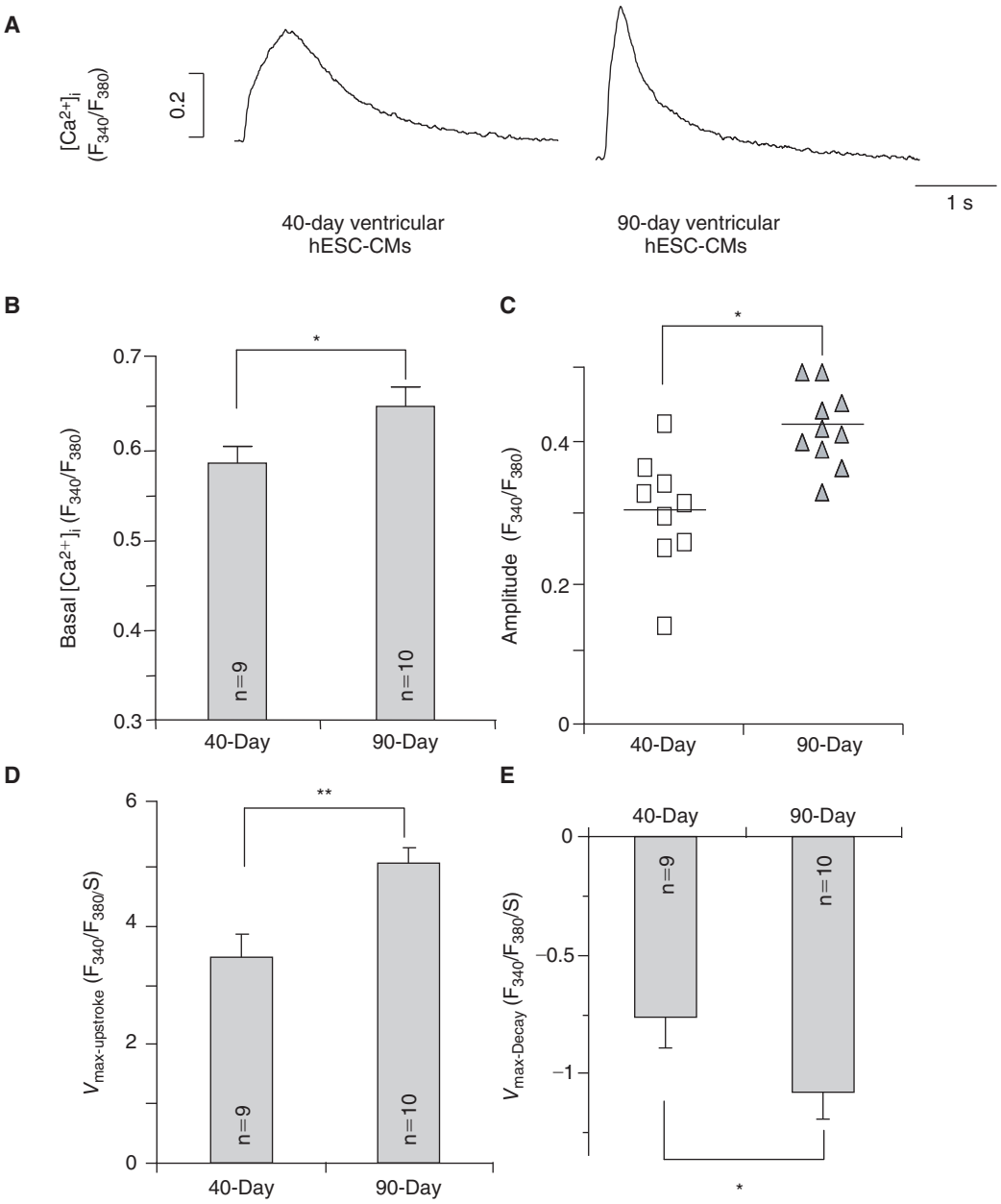

FIG. 2. Ca^{2+} transients recorded from 7+40- to 7+90-day dsRed+ ventricular hESC-CMs. (**A**) Representative tracings of Ca^{2+} transients. (**B**–**E**) Comparison of the basal $[Ca^{2+}]_i$ (**B**), amplitude (**C**), maximum upstroke velocity ($V_{max\text{-}upstroke}$, **D**), and maximum decay velocity ($V_{max\text{-}decay}$, **E**) of Ca^{2+} transients in 40-day ($n = 9$) and 90-day ($n = 10$) dsRed+ ventricular hESC-CMs. $^*P < 0.05$, $^{**}P < 0.01$.

was completely blocked by 10 μmol/L nifedipine (Fig. 3B). These results raise the possibility that additional source(s) of Ca^{2+} other than $I_{Ca\text{-}L}$ is present in ventricular hESC-CMs that suffice to initiate CICR.

Contribution of NCX to Ca^{2+} transients during human ventricular differentiation

To obtain molecular insights, we next analyzed the transcriptional expression levels of the three NCX isoforms (ie, NCX1, 2, and 3) in undifferentiated hESCs, hESC-derived ventricular (V) CMs, human fetal VCMs, and adult VCMs. Figure 4A shows that only the expression of NCX1, but not the other isoforms, increased during cardiac differentiation from hESCs to hESC-VCMs, peaked in fetal VCMs then decreased in adult VCMs. In our previous studies, we have also reported that the NCX1 is abundantly expressed in unsorted human ESC-CMs at the protein level [7]. However, it remains unknown whether I_{NCX} is functionally expressed in ventricular hESC-CMs. When operating in the reverse mode, the NCX current (I_{NCX}) can contribute to the elevation of cytosolic Ca^{2+} in early developing murine ESC-CMs [14] and fetal CMs [15]. Figure 4B shows that Ni^{2+} (5 mM), an inhibitor of NCX, completely abolished Ca^{2+} transients of dsRed+ ventricular hESC-CMs. To test for the functional expression of I_{NCX}, we voltage-clamped and compared

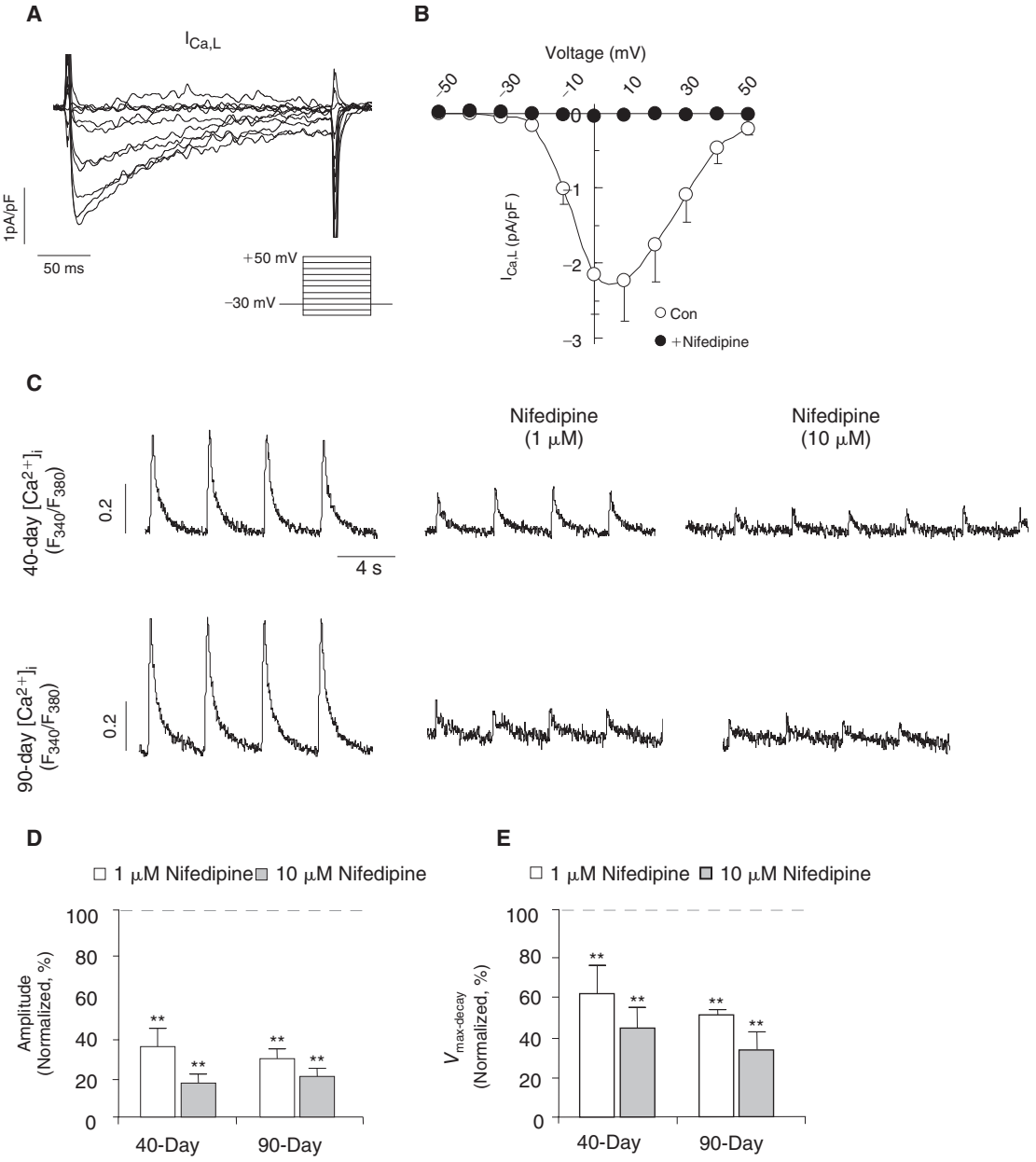

FIG. 3. The inhibitory effect of nifedipine on Ca^{2+} transients during ventricular hESC-CM differentiation. (**A**) L-type Ca^{2+} current ($I_{Ca,L}$) in 7+40-day dsRed+ ventricular hESC-CMs and (**B**) the corresponding current–voltage (I-V) relationship. (**C**) Representative tracings of Ca^{2+} transients in 7+40- and 7+90-day dsRed+ cells before and after nifedipine treatment. Bar graphs of normalized amplitude (**D**) and maximum upstroke velocity ($V_{max\text{-}upstroke}$, **E**) of Ca^{2+} transients after nifedipine. $^{**}P < 0.01$.

7+40- and 7+90-day dsRed+ ventricular hESC-CMs. Similar to previous studies, blockers for K^+, Ca^{2+}-activated Cl^-, and L-type Ca^{2+} currents, as well as the Na^+/K^+ pump, were added to isolate I_{NCX} [12]. Figure 4C shows that I_{NCX}, defined as Ni^{2+} (5 mM)-sensitive currents, was indeed functionally and robustly expressed in 7+40- and 7+90-day dsRed+ ventricular hESC-CMs. A voltage ramp from +60 to −120 mV elicited an almost linear current–voltage relationship of I_{NCX} (Fig. 4D), similar to those previously described for fetal and adult mouse CMs [15]. The I_{NCX} densities in 40-day ventricular hESC-CMs were -1.2 ± 0.6 pA/pF ($n = 4$) at −120 mV (Ca^{2+} outward mode) and 3.6 ± 1.0 pA/pF at 60 mV (Ca^{2+} inward mode). Significant increases of I_{NCX}, particularly in the Ca^{2+} outward mode, were observed in 90-day ventricular hESC-CMs (-6.9 ± 1.3 pA/pF or ~6-fold increase at −120 mV $n = 5$ and 7.9 ± 1.3 pA/pF or ~2-fold at 60 mV; $P < 0.05$).

To explore the functional role of I_{NCX} in Ca^{2+} transients of ventricular hESC-CMs, we next applied a Na^+-free external solution to prevent NCX from extruding Ca^{2+} [14,16]. Upon its perfusion, the basal $[Ca^{2+}]_i$ increased significantly in 7+90-day, but not 7+40-day, dsRed+ ventricular hESC-CMs (Fig. 5A and 5B). With a higher cytosolic $[Ca^{2+}]_i$, 7+90-day ventricular hESC-CMs spontaneously but irregularly fired Ca^{2+} transients upon a single stimulus (Fig. 5A). Detailed

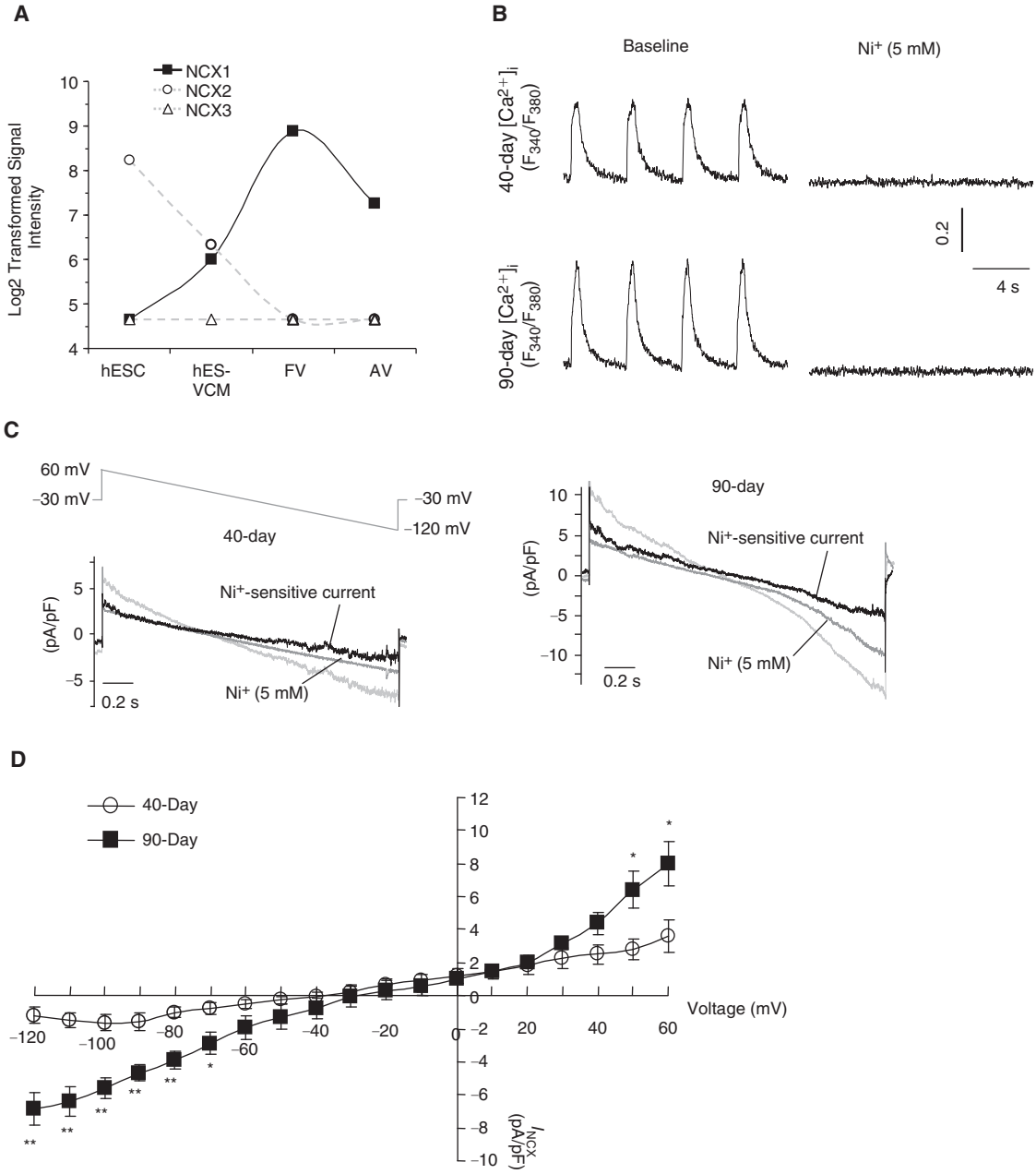

FIG. 4. Developmental changes of NCX current (I_{NCX}) in dsRed+ ventricular hESC-CMs. (**A**) The transcriptional expression of Na^+/Ca^{2+} exchanger (NCX) 1, NCX2, and NCX3 in hESCs, hESC-ventricular (V) CMs, fetal VCMs (FV), and adult VCMs (AV). (**B**) Representative tracings of Ca^{2+} transients in 7+40- and 7+90-day dsRed+ cells before and after Ni^+ treatment. (**C**) Protocol and typical tracings of I_{NCX}, and (**D**) I/V curve of I_{NCX} in 7+40- and 7+90-day dsRed+ cells. $^*P < 0.05$, $^{**}P < 0.01$.

analysis of the first Ca^{2+} transient elicited revealed that both its Ca^{2+} transient amplitude and decay velocity reduced to 76.8% ± 6.2% ($n = 4$, Fig. 5C) and 38.0% ± 13.9% ($n = 4$, Fig. 5D), respectively. Similarly, the Na^+-free solution decreased the amplitude (to 66.3% ± 5.8%, $n = 4$) and slowed the decay velocity (to 51.6% ± 16.4%, $n = 4$) of 7+40-day ventricular hESC-CMs, although irregular firing was not observed. Consistently, Ca^{2+} transients were completely blocked in both 7+40- and 7+90-day dsRed+ ventricular hESC-CMs cells only when both nifedipine and Na^+-free conditions were used. Upon reperfusion of the normal Tyrode solution (containing 140 mM Na^+) even in the presence of nifedipine (10 μmol/L), small Ca^{2+} transients could be elicited (Fig. 5E). Taken collectively, our results strongly suggest that the reverse mode of I_{NCX} contributes significantly to the Ca^{2+}-handling properties of developing ventricular hESC-CMs.

Discussion

It is now well-accepted that hESC-CMs differentiated from hESCs are highly heterogeneous consisting of ventricular-, atrial-, and pacemaker-like derivatives, fibroblasts, as well as extracardiac cell types. Technically, this heterogeneity has largely limited their functional characterization

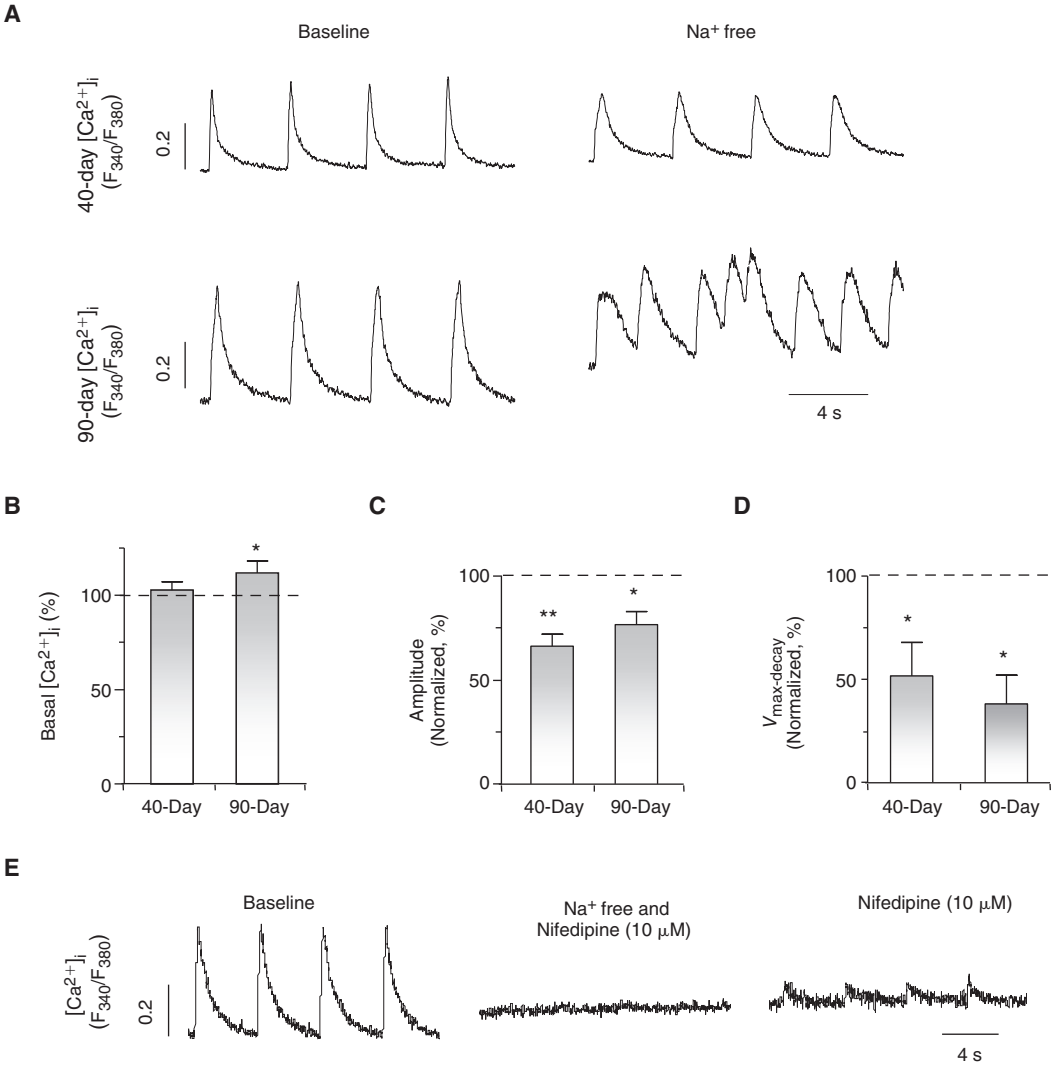

FIG. 5. I_{NCX} contributes to E-C coupling of ventricular hESC-CMs. (**A**) Representative tracings of Ca^{2+} transients in 40-day and 90-day dsRed+ cells with and without external Na^+. Normalized basal $[Ca^{2+}]_i$ (**B**), amplitude (**C**), and maximum decay velocity ($V_{max\text{-}decay}$, **D**) of Ca^{2+} transients in 7+40- and 7+90-day ventricular hESC-CMs after replacing with a Na^+-free external solution. $^*P < 0.05$; $^{**}P < 0.01$. (**E**) Ca^{2+} transients were completely blocked in ventricular hESC-CMs treated with nifedipine and Na^+-free solution.

and therefore, our understanding of their biology. Adding an extra level of complexity is the fact that although hESCs are by definition pluripotent, different lines have distinct cardiogenic potentials to become early ventricular-, atrial-, and pacemaker-like derivatives [3]. For instance, we have reported that HES2 cells have a high likelihood of differentiating into ventricular-like hESC-CMs while the atrial-like phenotype predominates in H1. Pacemaker-like hESCs were always the minority (<5%) [3]. Despite the different distributions, HES2-derived ventricular-, atrial-, and pacemaker-like derivatives display electrophysiological properties comparable to those of H1 once they are differentiated. As such, ambiguities exist if chamber-specific cells are not selected for experiments. In the present study, we employed the classical strategy that has been proven for mESCs [9,17] for purifying out ventricular hESC-CMs for experiments. Expression of dsRed under the transcriptional control of MLC2v appeared upon the occurrence of spontaneously beating activities and increased time-dependently; dsRed+ cells could be isolated and FACS-sorted into single cells. Patch-clamp recordings revealed an AP profile that is consistent with the ventricular phenotype. dsRed$^+$ hESC-CMs were positively immunostained for the cardiac-specific proteins cTnI and MHC (data not shown). Indeed, Huber et al. recently reported a similar strategy to identify hESC-derived ventricular derivatives by expressing GFP under the transcriptional control of the MLC2v promoter although the functional properties of their labeled derivatives were not studied and reported [18].

Compared to adult CMs, fetal CMs have smaller Ca^{2+} transient amplitudes and slower dynamics, and display developmental changes during the maturation process [11]. In rat and rabbit, cardiac sarcolemmal NCX is abundantly expressed and functionally well-developed in late fetal, reaches a maximum at perinatal, followed by declining at adult stages [19,20]. In developing mouse embryonic CMs, functional NCX operates in both Ca^{2+} inward and outward

modes to maintain intracellular Ca^{2+} homeostasis also with a significantly higher basal NCX current (I_{NCX}) density at early (10.5 dpc) than late (16.5 dpc) stages [15]. Haddock et al. report that Ca^{2+} entry via outward I_{NCX} directly supports contraction of newborn rabbit ventricular myocytes [21]. Along the same line, both NCX transcript and protein levels have been recently shown to increase from 10-week to 20-week gestation during human heart development, then decrease at neonate and further diminish at adult stages [22]. Consistently, the same expression pattern was observed in our own study. We have previously reported that the cardiac NCX1 protein is abundantly expressed in human fetal ventricular and hESC-CMs [7]. Using MLC2v-dsRed hESCs, here we further showed that NCX is indeed functionally expressed in ventricular hESC-CMs. Developmentally, I_{NCX}, particularly the outward mode, increases time-dependently, consistent with the higher NCX transcript and protein expression levels in human fetal heart [7,22]. Given the relatively low NCX level in adult, it is reasonable to extrapolate from these findings that NCX continues to increase during cardiogenesis and declines only after the fetal stage to reach the adult level as part of the maturation process. Taken collectively, our results and those of others have revealed significant evolutionary footprints, as well as differences, between human and various mammalian species.

In adult CMs, E-C coupling is initiated primarily by CICR. $I_{Ca\text{-}L}$ serves as the major source of Ca^{2+} influx to trigger Ca^{2+} release from the SR. With immature SR [7], E-C coupling of developing hESC-CMs is anticipated to particularly depend on sarcolemmal Ca^{2+} influx. Consistent with this notion, our results show that $I_{Ca\text{-}L}$ functions and plays an important role in E-C coupling of ventricular hESC-CMs: >80% Ca^{2+} transients were inhibited in 7+40- and 7+90-day ventricular hESC-CMs when $I_{Ca\text{-}L}$ was completely blocked by nifedipine. As for the residual transient, we identified I_{NCX} as the alternative source of Ca^{2+} influx for triggering CICR or E-C coupling [23,24]. Depending on the transmembrane potential and the electrochemical gradients of substrate ions, I_{NCX}, as a bidirectional transporter, can be inward or outward to mediate the extrusion or influx of Ca^{2+} ions, respectively [25]. Indeed, NCX is known to contribute to both contraction and relaxation of CMs. Under physiological conditions (high external Na^+), the Ca^{2+} outward mode of NCX plays a crucial role in maintaining a low resting cytosolic Ca^{2+} after systole [26]; when intracellular Na^+ ions start to accumulate (eg, during AP when Na^+ channels open), the NCX can operate in the reverse mode to transport Ca^{2+} from the outside to the inside while exporting Na^+. This reverse mode NCX has been thought to synergize $I_{Ca\text{-}L}$ to trigger SR Ca^{2+} release in adult myocytes [23,24], and contribute to the slow Ca^{2+} transient decay observed in failing heart cells [27,28]. A similar mechanism has also been reported to trigger the Ca^{2+} release from intracellular Ca^{2+} stores in cultured cortical neurons [29]. Functionally, acute blockade of NCX by removing extracellular Na^+ significantly increased the basal cytosolic Ca^{2+} and inhibited Ca^{2+} transients in ventricular hESC-CMs. Indeed, spontaneous but irregular firing Ca^{2+} transients were even induced in 7+90-day ventricular cells, which could be attributed to increased Ca^{2+} sparks [16] and predispose to arrhythmias. Recently, NCX has been reported to co-localize with ryanodine receptor (RyR) in neonatal rabbit ventricular myocytes [30], and its reverse mode is functionally coupled to RyR to initiate CICR with attenuated efficacy with ontogeny [31]. Of note, species-dependent differences exist for NCX function during development. Ca^{2+} influx by NCX contributes to Ca^{2+} transients even in early-stage differentiated hESC-CMs, although NCX exerts no effects on Ca^{2+} transients in early-stage mouse ESC-CMs [14].

Pluripotent hESC-like iPSCs have been recently derived by reprogramming adult somatic (fibroblast) cells [32,33]. Using protocols originally developed for maintaining and cardiac differentiation of hESCs, iPSC can be similarly cultured and differentiated into CMs. iPSC-CMs express key cardiac-specific proteins, and spontaneously contract in a manner similar to hESC-CMs, and are also heterogeneous with nodal-, atrial-, and ventricular-like phenotypes [34]. Our MLC2v-dsRed-based selection strategy will be useful for characterizing and comparing ventricular iPSC- and hESC-CMs. A better understanding of the basic biology of ventricular derivatives is crucial for their ultimate clinical application in myocardial repair. Additionally, although the Ca^{2+}-handling properties of ventricular hESC-CMs appear to mature in culture in vitro, they did not reach the adult level even after 100 days. The results further implicate that alternative protocols need to be developed for facilitating functional maturation to improve both the safety and efficacy of hESC-CMs.

Conclusion

We have generated the stably LV-transduced MLC2v-dsRed hESC line and electrophysiologically characterized their dsRed+ ventricular derivatives. Based on our present results, we conclude that NCX is functionally expressed in, and contributes to their Ca^{2+}-handling properties of ventricular hESC-CMs.

Acknowledgments

This work was supported by grants from the National Institutes of Health—R01 HL72857 (to R.A.L.), the Stem Cell Program of the University of California (to R.A.L.), the California Institute for Regenerative Medicine (to J.D.F. and R.A.L.), and the CC Wong Foundation Stem Cell Fund (to R.A.L.).

Author Disclosure Statement

No competing financial interests exist.

References

1. He JQ, Y Ma, Y Lee, JA Thomson and TJ Kamp. (2003). Human embryonic stem cells develop into multiple types of cardiac myocytes: action potential characterization. Circ Res 93:32–39.
2. Xue T, HC Cho, FG Akar, SY Tsang, SP Jones, E Marbán, GF Tomaselli and RA Li. (2005). Functional integration of electrically active cardiac derivatives from genetically engineered human embryonic stem cells with quiescent recipient ventricular cardiomyocytes: insights into the development of cell-based pacemakers. Circulation 111:11–20.
3. Moore JC, J Fu, YC Chan, D Lin, H Tran, HF Tse and RA Li. (2008). Distinct cardiogenic preferences of two human embryonic stem cell (hESC) lines are imprinted in their proteomes in the pluripotent state. Biochem Biophys Res Commun 372:553–558.
4. Bers DM and CR Weber. (2002). Na/Ca exchange function in intact ventricular myocytes. Ann N Y Acad Sci 976:500–512.
5. Wakimoto K, K Kobayashi, M Kuro-O, A Yao, T Iwamoto, N Yanaka, S Kita, A Nishida, S Azuma, Y Toyoda, K Omori, H

Imahie, T Oka, S Kudoh, O Kohmoto, Y Yazaki, M Shigekawa, Y Imai, Y Nabeshima and I Komuro. (2000). Targeted disruption of Na^+/Ca^{2+} exchanger gene leads to cardiomyocyte apoptosis and defects in heartbeat. J Biol Chem 275:36991–36998.
6. Koushik SV, J Wang, R Rogers, D Moskophidis, NA Lambert, TL Creazzo and SJ Conway. (2001). Targeted inactivation of the sodium-calcium exchanger (Ncx1) results in the lack of a heartbeat and abnormal myofibrillar organization. FASEB J 15:1209–1211.
7. Liu J, JD Fu, CW Siu and RA Li. (2007). Functional sarcoplasmic reticulum for calcium handling of human embryonic stem cell-derived cardiomyocytes: insights for driven maturation. Stem Cells 25:3038–3044.
8. Henderson SA, M Spencer, A Sen, C Kumar, MA Siddiqui and KR Chien. (1989). Structure, organization, and expression of the rat cardiac myosin light chain-2 gene. Identification of a 250-base pair fragment which confers cardiac-specific expression. J Biol Chem 264:18142–18148.
9. Müller M, BK Fleischmann, S Selbert, GJ Ji, E Endl, G Middeler, OJ Müller, P Schlenke, S Frese, AM Wobus, J Hescheler, HA Katus and WM Franz. (2000). Selection of ventricular-like cardiomyocytes from ES cells in vitro. FASEB J 14:2540–2548.
10. Moore JC, R Spijker, AC Martens, T de Boer, MB Rook, MA van der Heyden, LG Tertoolen and CL Mummery. (2004). A P19Cl6 GFP reporter line to quantify cardiomyocyte differentiation of stem cells. Int J Dev Biol 48:47–55.
11. Fu JD, J Li, D Tweedie, HM Yu, L Chen, R Wang, DR Riordon, SA Brugh, SQ Wang, KR Boheler and HT Yang. (2006). Crucial role of the sarcoplasmic reticulum in the developmental regulation of Ca^{2+} transients and contraction in cardiomyocytes derived from embryonic stem cells. FASEB J 20:181–183.
12. Artman M, H Ichikawa, M Avkiran and WA Coetzee. (1995). Na^+/Ca^{2+} exchange current density in cardiac myocytes from rabbits and guinea pigs during postnatal development. Am J Physiol 268(4 Pt 2):H1714–H1722.
13. Patton C, S Thompson and D Epel. (2004). Some precautions in using chelators to buffer metals in biological solutions. Cell Calcium 35:427–431.
14. Fu JD, HM Yu, R Wang, J Liang and HT Yang. (2006). Developmental regulation of intracellular calcium transients during cardiomyocyte differentiation of mouse embryonic stem cells. Acta Pharmacol Sin 27:901–910.
15. Reppel M, P Sasse, D Malan, F Nguemo, H Reuter, W Bloch, J Hescheler and BK Fleischmann. (2007). Functional expression of the Na^+/Ca^{2+} exchanger in the embryonic mouse heart. J Mol Cell Cardiol 42:121–132.
16. Goldhaber JI, ST Lamp, DO Walter, A Garfinkel, GH Fukumoto and JN Weiss. (1999). Local regulation of the threshold for calcium sparks in rat ventricular myocytes: role of sodium-calcium exchange. J Physiol (Lond) 520(Pt 2):431–438.
17. Klug MG, MH Soonpaa, GY Koh and LJ Field. (1996). Genetically selected cardiomyocytes from differentiating embronic stem cells form stable intracardiac grafts. J Clin Invest 98:216–224.
18. Huber I, I Itzhaki, O Caspi, G Arbel, M Tzukerman, A Gepstein, M Habib, L Yankelson, I Kehat and L Gepstein. (2007). Identification and selection of cardiomyocytes during human embryonic stem cell differentiation. FASEB J 21:2551–2563.
19. Artman M. (1992). Sarcolemmal $Na(+)$-Ca^{2+} exchange activity and exchanger immunoreactivity in developing rabbit hearts. Am J Physiol 263(5 Pt 2):H1506–H1513.
20. Koban MU, AF Moorman, J Holtz, MH Yacoub and KR Boheler. (1998). Expressional analysis of the cardiac Na-Ca exchanger in rat development and senescence. Cardiovasc Res 37:405–423.
21. Haddock PS, WA Coetzee and M Artman. (1997). Na^+/Ca^{2+} exchange current and contractions measured under Cl(-)-free conditions in developing rabbit hearts. Am J Physiol 273(2 Pt 2):H837–H846.
22. Qu Y, A Ghatpande, N el-Sherif and M Boutjdir. (2000). Gene expression of Na^+/Ca^{2+} exchanger during development in human heart. Cardiovasc Res 45:866–873.
23. Levesque PC, N Leblanc and JR Hume. (1991). Role of reverse-mode $Na(+)$-Ca^{2+} exchange in excitation-contraction coupling in the heart. Ann N Y Acad Sci 639:386–397.
24. Litwin SE, J Li and JH Bridge. (1998). Na-Ca exchange and the trigger for sarcoplasmic reticulum Ca release: studies in adult rabbit ventricular myocytes. Biophys J 75:359–371.
25. Blaustein MP and WJ Lederer. (1999). Sodium/calcium exchange: its physiological implications. Physiol Rev 79:763–854.
26. Barcenas-Ruiz L, DJ Beuckelmann and WG Wier. (1987). Sodium-calcium exchange in heart: membrane currents and changes in $[Ca^{2+}]_i$. Science 238:1720–1722.
27. Dipla K, JA Mattiello, KB Margulies, V Jeevanandam and SR Houser. (1999). The sarcoplasmic reticulum and the Na^+/Ca^{2+} exchanger both contribute to the Ca^{2+} transient of failing human ventricular myocytes. Circ Res 84:435–444.
28. Weisser-Thomas J, V Piacentino III, JP Gaughan, K Margulies and SR Houser. (2003). Calcium entry via Na/Ca exchange during the action potential directly contributes to contraction of failing human ventricular myocytes. Cardiovasc Res 57:974–985.
29. Wu MP, LS Kao, HT Liao and CY Pan. (2008). Reverse mode Na^+/Ca^{2+} exchangers trigger the release of Ca^{2+} from intracellular Ca^{2+} stores in cultured rat embryonic cortical neurons. Brain Res 1201:41–51.
30. Dan P, E Lin, J Huang, P Biln and GF Tibbits. (2007). Three-dimensional distribution of cardiac Na^+-Ca^{2+} exchanger and ryanodine receptor during development. Biophys J 93:2504–2518.
31. Huang J, L Hove-Madsen and GF Tibbits. (2008). Ontogeny of Ca^{2+}-induced Ca^{2+} release in rabbit ventricular myocytes. Am J Physiol, Cell Physiol 294:C516–C525.
32. Yu J, MA Vodyanik, K Smuga-Otto, J Antosiewicz-Bourget, JL Frane, S Tian, J Nie, GA Jonsdottir, V Ruotti, R Stewart, II Slukvin and JA Thomson. (2007). Induced pluripotent stem cell lines derived from human somatic cells. Science 318:1917–1920.
33. Takahashi K, K Tanabe, M Ohnuki, M Narita, T Ichisaka, K Tomoda and S Yamanaka. (2007). Induction of pluripotent stem cells from adult human fibroblasts by defined factors. Cell 131:861–872.
34. Zhang J, GF Wilson, AG Soerens, CH Koonce, J Yu, SP Palecek, JA Thomson and TJ Kamp. (2009). Functional cardiomyocytes derived from human induced pluripotent stem cells. Circ Res 104:e30–e41.

Address correspondence to:
Dr. Ronald Li
University of California Davis
Room 650
Shriners Hospital
2425 Stockton Blvd.
Sacramento, CA 95817

E-mail: ronaldli@ucdavis.edu

Received for publication May 27, 2009
Accepted after revision August 31, 2009
Prepublished on Liebert Instant Online August 31, 2009